

# The Interface Structure in Dissimilar Welding of AISI 4130 to AISI 316L Steels Using ERNiCr-3 Filler Metal

H. Mostaan <sup>\*1</sup>, M. Poorkabirian <sup>2</sup>, M. Rafiei <sup>3</sup>

<sup>1</sup> Department of Materials and Metallurgical Engineering, Faculty of Engineering, Arak University, arak, Iran

<sup>2,3</sup> Advanced Materials Research Center, Department of Materials Engineering, Najafabad Branch, Islamic Azad University, Najafabad, Iran

## Abstract

In this research the interface structure of dissimilar joint between AISI 4130 and AISI 316L steels produced by GTAW process was evaluated. ERNiCr-3 was used as a filler metal for this joint. After welding the microstructure of different areas including weld metals, heat affected zones and interfaces were studied by optical microscope (OM), scanning electron microscope (SEM) and energy dispersive spectroscopy (EDS) analysis. It was found that the weld metal entirely has austenitic microstructure with relatively equiaxed grains and dendritic morphology. The results also showed that the grain growth in 4130 steel-weld metal interface was unepitaxial due to the severe difference in chemical composition between the base and weld metals. Microhardness measurements showed that the welded sample indicated the highest microhardness in the heat affected zone of 4130 steel because of the presence of tempered martensite and bainite in this area. In the weld zone a decrease in hardness value from AISI 4130 steel to AISI 316L can be seen. This reduction in microhardness can be due to the less amount of carbon in the weld area in vicinity of the AISI 316L base metal.

**Keywords:** Dissimilar Joint; GTAW; 316L Steel; 4130 Low alloy steel; ERNiCr-3; Interface structure.

## 1. Introduction

The AISI 4130 steel is a heat treatable low alloy steel (HTLA). It is of medium carbon steel and includes alloy elements such as chromium, molybdenum, manganese and other elements <sup>1-4</sup>. This type of steel is used in the oil industry and power plants. In addition, due to the oxidation resistance and very good strength at high temperatures, it is used in a variety of generators and heat exchangers <sup>4</sup>. Heat treatable low alloy steel is used in

normalized, quenched and tempered states. Chromium element in this steel increases corrosion resistance and high temperature strength of this steel. molybdenum is also used for preventing the pitting corrosion <sup>3</sup>. 316L stainless steel after 304 stainless steel is the second most common austenitic stainless steel <sup>5</sup>. This is also known as marine grade stainless steel and usually contains 16% chromium, 10% nickel and 2% molybdenum <sup>5</sup>.

The change in ratio of chrome, nickel and molybdenum of 316L steel Compared to other stainless steels increases the corrosion resistance especially in chloride environments <sup>5,6</sup>. This property extends the application of these steels in corrosive environments.

316L stainless steel is used in various industries such as oil, gas, petrochemical, pharmaceutical, food industries, etc. Also this alloy is used for the manufacturing of pipes and sheets in acidic environments and its price is more expensive compared with 304 stainless steel <sup>5</sup>.

Dissimilar welding of stainless steel and heat treatable low alloy steel with high strength has plenty of appli-

\* Corresponding author

Email: h-mostaan@araku.ac.ir

Address: Department of Materials and Metallurgical Engineering, Faculty of Engineering, Arak University, arak, Iran

1. Assistant Professor

2. M.Sc.

3. Assistant Professor

cations in a variety of industries such as oil, gas, petrochemical, thermal power plants and the food industry <sup>7, 8)</sup>.

In the most of the mentioned industries, the fluid transfer tube lines and nozzles are made of stainless steel. Also tanks and under pressure parts of the systems are made of heat treatable low alloy steels and the welding methods to joint these components are of the most important existing joints in these industries <sup>9)</sup>.

Due to the extensive application of heat treatable low alloy and stainless steels in various industries and abundant needs to joint these two types of steels to each other, developing and optimizing the properties of this joint has always been the critical case. In the past, some research has been done concerning the application of various filler metals for this joint.

Panyndra et al. <sup>8)</sup> used GTAW method for investigating the properties of dissimilar welding of AISI 4140 to AISI 316 steels. They used two methods, without and with filler metal. The used filler metal was ER309L. The results showed that the properties of dissimilar joint in both cases were acceptable.

Jang et al. <sup>9)</sup> examined the structure and mechanical properties of the joints between SA 508 steel and 316 stainless steel with inconel182/82 as the filler metal by GTAW process. In this research the microstructure and mechanical properties of the joint were different through the welding thickness. Also in this research the residual stress was responsible for the crack formation in the welded samples.

Kim et al. <sup>10)</sup> did a similar research to Zhang et al. <sup>9)</sup> and used post weld heat treatment (PWHT) process at 320 oC for reducing the residual stress in the welded samples. These authors indicated that the PWHT process had a great effect on reducing the residual stress. Also they reported that the welding structure was dendritic and the fracture surface of the welded samples was ductile.

Aryvazhagan et al. <sup>7)</sup> examined the joint properties of AISI 4140 steel to AISI 304 using GTAW, Friction welding (FRW) and electron beam welding (EBW). The results showed that the method of welding had a great effect on mechanical properties of the joint. The joint created by electron beam welding (EBW) indicated the highest tensile strength and the joint created by GTAW

method showed maximum impact resistance.

Among different methods of fusion welding processes, one of the most common methods is GTAW welding. This method has several benefits and create a clean weld zone. <sup>3, 11)</sup> GTAW process compared to other advanced techniques such as electron beam welding (EBW) and laser beam welding (LBW) has some weaknesses, for example, low penetration depth, extended HAZ and higher distortion in thin sheets <sup>3, 12)</sup>.

To improve the GTAW welding properties, Ahmadi and Ebrahimi <sup>11)</sup> studied the effect of flux in permeation depth of GTAW welding in 316L stainless steel and the results showed an increase in the permeation depth.

Chandran et al. <sup>13)</sup> investigated the effect of welding parameters on toughness and hardness in the joint of AISI 4140 steel to AISI 304 stainless steel using friction welding process. The main investigated parameters were frictional force and the pressing force. The share of each of the parameters and the importance of these parameters were determined by Taguchi method and the results showed that frictional force had the most effect in the toughness of the joint.

Özdemir et al. <sup>14)</sup> studied the effect of spin speed in the joint properties of friction welding of AISI 304 to AISI 4340 steels. Friction welding was performed using a device with five different spin speeds. It was observed that the tensile strength increased by increasing the rotation speed.

Regarding the mentioned research it was found that there was no study about the welding of AISI 4130 to AISI 316L steels with ERNiCr-3. Therefore, the aim of this research is to study the microstructure and interfaces of the dissimilar joint between AISI 4130 to AISI 316L steels.

## 2. Materials and Procedures

### 2.1. Materials

In this research, the heat treatable low alloy (HTLA) steel sheet of AISI 4130 and AISI 316L austenitic stainless steel sheet were used. Quantometry analysis was performed to determine the exact chemical composition of the prepared sheets. The chemical composition of the base metals and the used filler metal are given in Table 1.

Table 1. The chemical composition of the base and filler metals (wt.%).

	Fe	C	Si	Mn	Cr	Mo	Ni	Cu	Al	Nb+Ta	Ti
<b>AISI 4130</b>	97.2	0.249	0.43	0.547	0.708	0.219	0.021	0.065	0.032	-	-
<b>AISI 316L</b>	67.7	0.051	0.497	1.83	17.4	1.97	9.52	0.485	0.485	-	-
<b>ER NiCr-3</b>	3.0	0.1	0.5	2.5 - 3.5	18 - 22	-	+Co 67	-	-	2-3	0.75

For welding the base metals, Inconel 82 (ERNiCr-3) was used as filler metal with diameter of 2.4 mm for all passes. This filler metal was selected because this filler metal includes high values of nickel and the goals were to create austenite microstructure and flexible weld zone.

In order to choose appropriate filler metals, some properties such as chemical composition, ultimate mechanical properties, thermal stability, corrosion resistance, thermal expansion coefficient and its cost were the main factors. Therefore, AWS A5.14 and AWS A5.9 standards and given specifications by the manufacturer were used.

## 2. 2. Sample preparation

In this research, two sheets of base metals (AISI 316L austenitic stainless steel and AISI 4130 low alloy steel) with dimensions of  $6 \times 70 \times 300 \text{ mm}^3$  were used. According to Fig. 1, the joint design was one-sided V-shaped configuration (this preparation was conducted according to AWS D1.1 standard).

As shown in Fig. 1, the bevel angle was set at  $50^\circ$ . The sand blasting, degreasing and cleaning processes were done before the welding in order to prevent formation of any defect such as lack of fusion or hydrogen induced cracking.

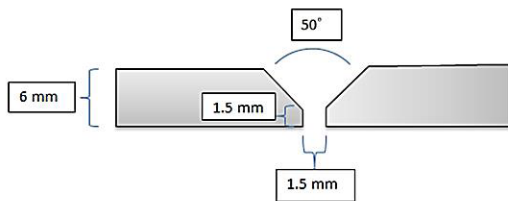


Fig. 1. The joint design of the sheets before welding.

## 2. 3. Welding process

Samples were welded using Inconel 82(ERNiCr-3) filler metal with a diameter of 2.4 mm. GTAW process was conducted using an ESAB DTA 300 device without preheating of the samples. In all cases, DCEN polarity and 1G position were used. The welding voltage and amperage were set at 15 V and 150-220 A respectively.

Tungsten electrode containing 2% thorium was used. Argon gas with 99.9% purity and the pressure of 4 to 5 bar was used as shielding atmosphere. Welding was performed in two passes and interpass temperature of about  $100^\circ \text{C}$  was chosen in order to minimize the residual stresses after welding.

## 2. 4. Microstructure observations

In order to study the microstructure of different areas i.e. weld metals, heat-affected zone (HAZ) and their interfaces and also the changes of microstructure, metallo-

graphic methods were used by the use of optical microscopy. The samples were cut in the dimensions of  $15 \times 30 \text{ mm}^2$ . Grinded and polished samples were prepared with semi-automatic machines according to ASTM E3-11 standard. After preparation process, the samples were etched with etching Nital solution (alcohol and nitric acid), Glysergia ( $\text{HCl} + \text{Glycerol} + \text{HNO}_3$ ) and Brahma color etching solutions (water-  $\text{K}_2\text{S}_2\text{O}_5$ -sulfamic acid-  $\text{NH}_4\text{F} \cdot \text{HF}$ ) according to ASTM E 407-2015 standard.

## 2. 5. Microhardness measurements

To study the mechanical properties of the joint, the Vickers microhardness tests were applied on samples along the width of the weld, in cross-sections of the samples according to the ASTM E-92 standard.

## 3. Results and Discussion

### 3. 1. The microstructure of the base metals

Fig. 2 shows optical microscope images of the microstructure of 4130 steel. The microstructure of 4130 steel contains bainite, ferrite and pearlite phases. This alloy is usually welded in the annealed or tempered state except in repair welding cases. In this case, annealing and tempering before welding are not acceptable<sup>3)</sup>.

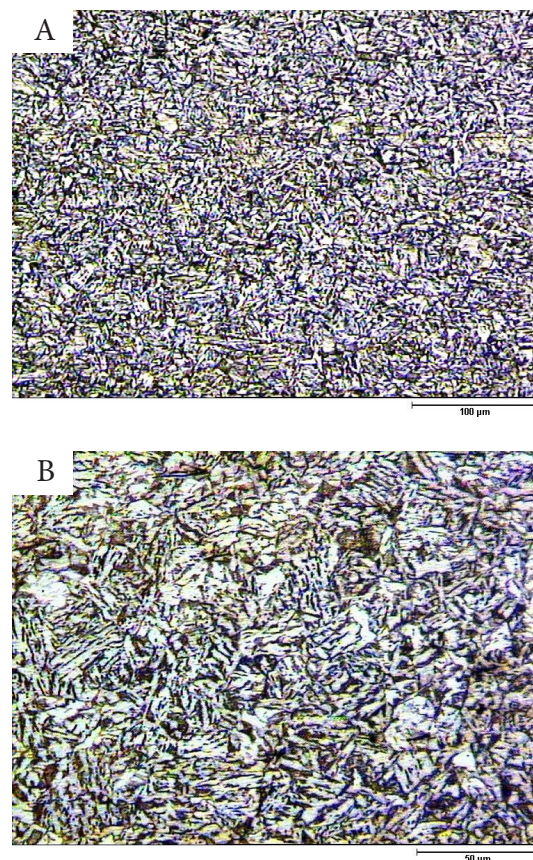


Fig. 2. The microstructure of AISI 4130 base metal at different magnifications.

Fig. 3 presents optical microscope images of the microstructure of AISI 316L austenitic stainless steel. The microstructure of 316L stainless steel consists of austenitic matrix and strings of delta ferrite. The grains were equiaxed and annealing twin boundaries were obviously seen in the structure. This structure is a result of annealing after cold rolling process. This process enhances the corrosion resistance and ductility of the alloy<sup>5, 15, 16, 17</sup>.

In Fig. 3, the existence of delta ferrite is clear. This delta ferrite accelerates the formation of sigma phase in the alloy after long-term exposure at 600 to 900 °C temperature rang<sup>3, 17</sup>.

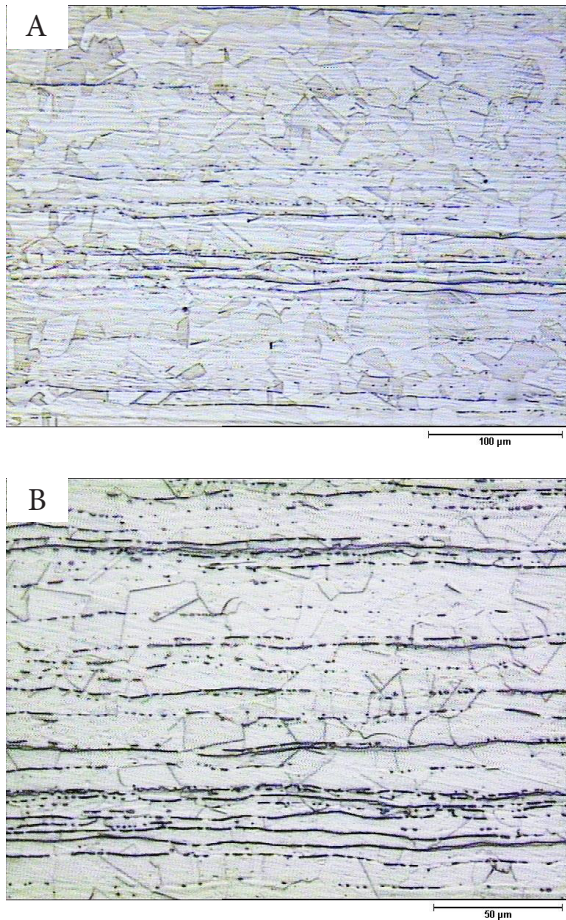


Fig. 3. The microstructure of 316L stainless steel base metal with different magnifications.

### 3. 2. Microstructure of the weld metal

As said above, the used filler metal for welding in this research was Inconel 82 (ERNiCr-3). The grain structure of the weld metal is shown in Fig. 4. As expected, microstructure is entirely austenitic and composed of relatively equiaxed grains. In Fig. 4, the cellular-dendritic structure is dominant and dendritic arms are clearly seen. Although equiaxed dendrites can be seen in some grains, orientation of dendritic growth in each grain is different. In fact a competitive growing structure is visible.

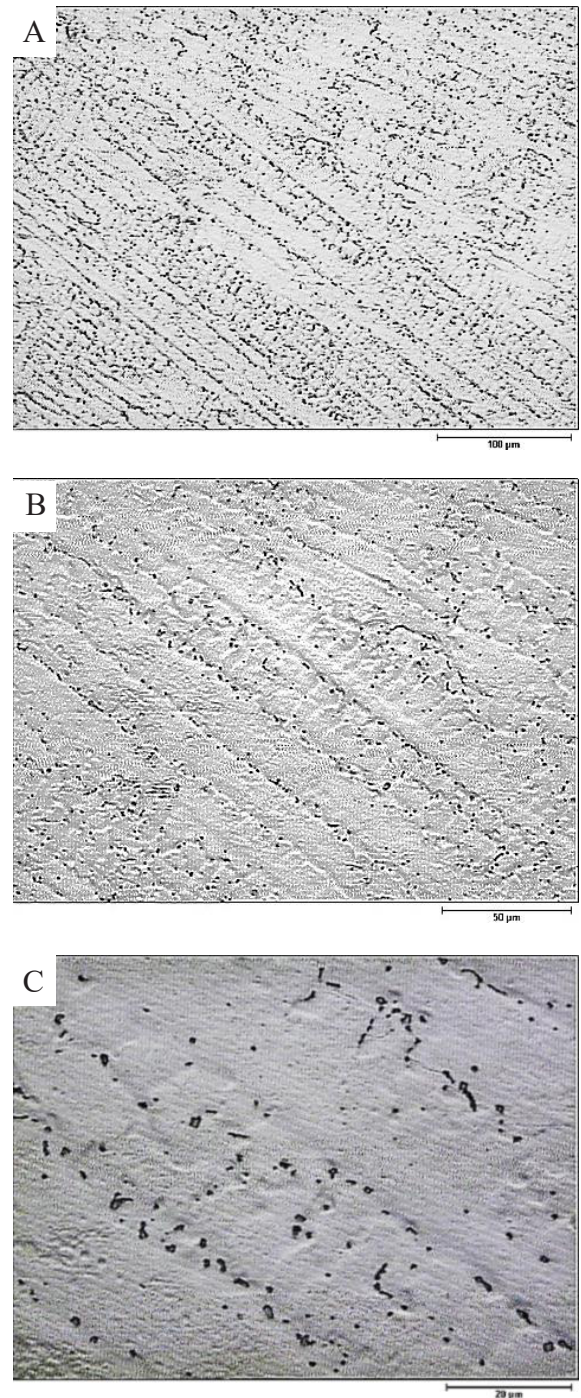


Fig. 4. The microstructure of the weld metal (INCONEL 82) at different magnifications.

### 3. 3. Interface microstructure

In this section, the grain structure, the mechanisms of grain solidification, grain growth and the boundaries morphology were investigated. Two different interfaces were discussed in this section. The first interface was between the weld metal and 4130 low alloy steel base metal and the second one was between 316L stainless steel base metal and the weld metal. These interfaces were studied separately.

In Fig. 5, the interface of 4130 steel and the weld metal has been shown. The HAZ structure contains ferrite, bainite and tempered martensite and welding zone has completely an austenitic structure. In this micrograph, the interface microstructure before etching of weld zone is observed (Fig. 5). At the weld zone and in the vicinity of the interface, a darker area can be seen. It can be said that in this area the amount of carbon is higher than other welding areas. This is due to the carbon migration from the 4130 steel to weld metal<sup>7, 17</sup>. In this area due to the high rate of heat transfer and rapid solidification, there is no possibility for formation of carbide phases. Therefore, the dissolved carbon content in this zone is high.

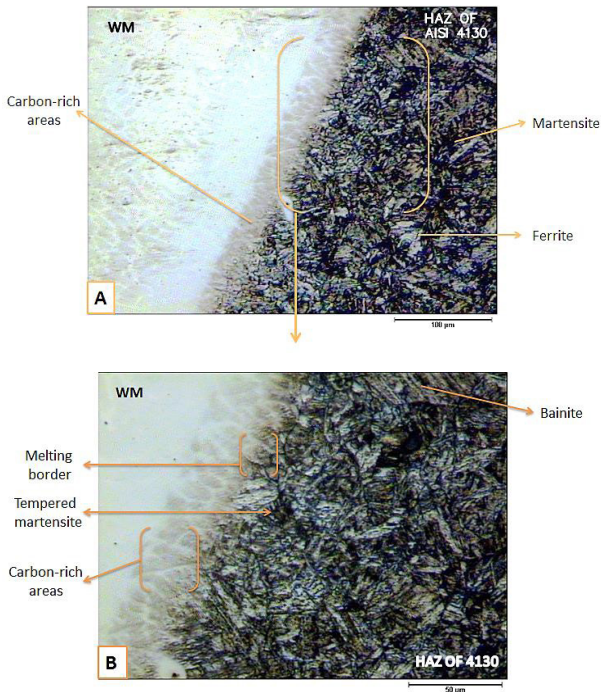


Fig. 5. The microstructure of 4130 steel-weld metal interface at different magnifications.

In Fig. 6 the microstructure of interface after etching of the weld zone is presented. In this image, cellular growth and columnar grains are clear. In addition, the solidification subgrain boundaries (SSGB), solidification grain boundaries (SGB) and migrated grain boundaries (MGB) can be seen. All these boundaries are due to the A type solidification mechanism (primary austenite). In Fig. 6 A and B, an unmixed zone in the interface is observed. This is due to the high difference in composition and crystal structure between base and weld metal and also poor mixing of the melted area in vicinity of the interface with weld metal. As mentioned previously, in the weld metal near the interface, no carbide particles can be seen. In Fig. 6, a competitive growth in the weld zone is seen. cellular growth and columns can be seen but the grain growth in this area is non-epitaxial.

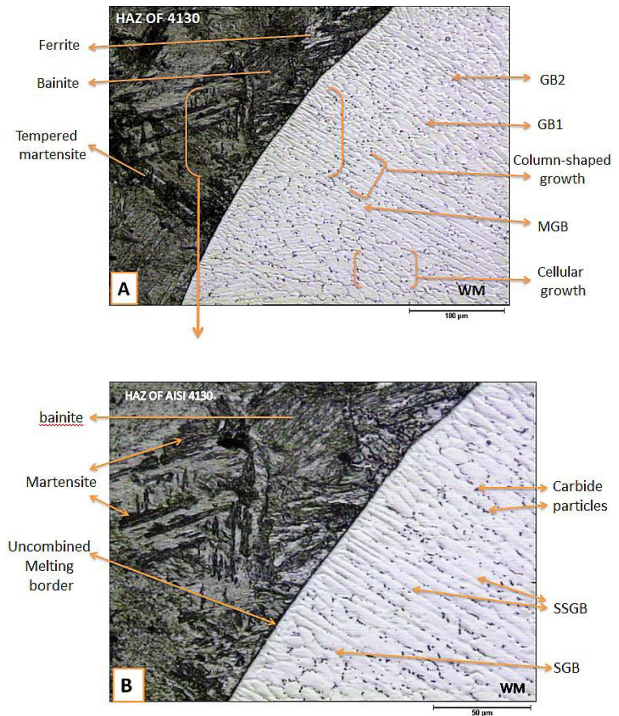


Fig. 6. The microstructure of 4130 steel-weld metal interface after etching of weld metal at different magnifications.

According to Fig. 7 (A), dendritic growth in some areas of weld zone is obvious. Whereas in Fig. 7 (B), flat growth area was seen. This area is due to the high rate of heat transfer and absence of constitutional undercooling. In this region, unlike other regions of the weld zone, carbide particles were not observed. Away from the fusion line dendritic and cellular solidification morphology were seen.

As said, in Figs. 6 and 7, an unmixed zone was formed in the vicinity of the fusion line. All these images were from the first pass of the welding process, but Fig. 8 which is from the second pass and fusion line is completely different.

In Fig. 8, a mixed fusion line and epitaxial growth in the vicinity of the interface can be seen. This is due to the different composition of the weld metal in the second pass, because of dilution changes in this pass and relatively similar composition of the weld and base metals.

In all metallography images, carbide particles can be seen in the weld zone. After analysis by EDS, as shown in Figs. 7 & 8, it was found that these particles are rich in Nb. Fig. 9 shows EDS analysis of carbide particles. The presence of these carbide particles in the grain boundary, prevents the grain growth. These carbide particles can increase the strength and hardness of the weld zone.

To study the changes of alloying elements, the line scan was used and the results are presented in Fig. 10. As seen drastic changes in alloying elements with severe slope at diagram, especially in the chromium and nickel in the interface, are visible.

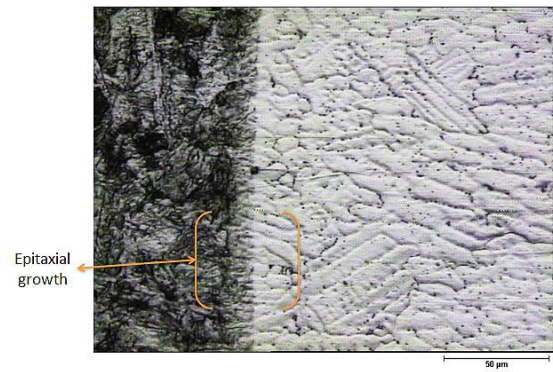
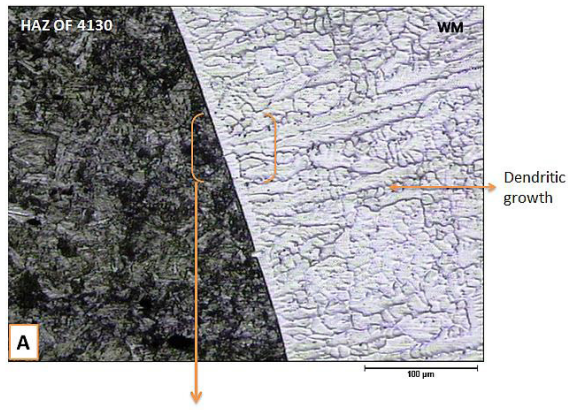


Fig. 8. The microstructure of 4130 steel-weld metal interface in the second pass.

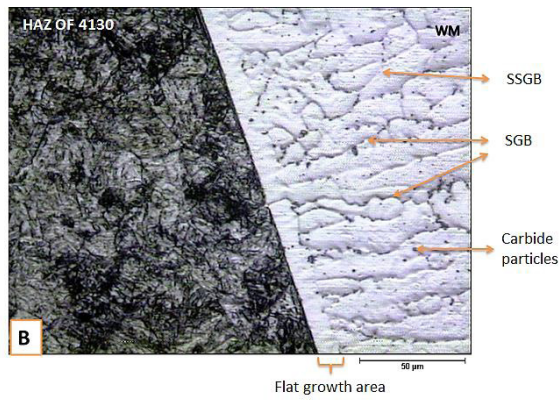


Fig. 7. The microstructure of 4130 steel-weld metal interface at different magnifications.

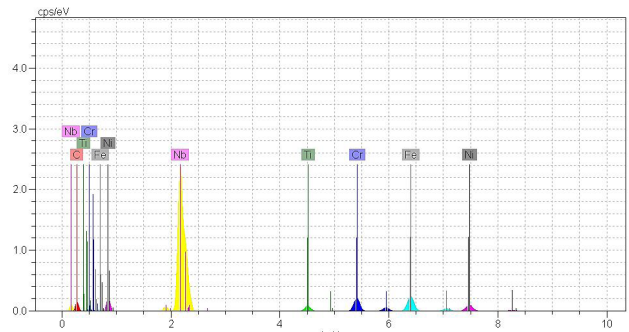


Fig. 9. The results of EDS analysis of carbide particles.

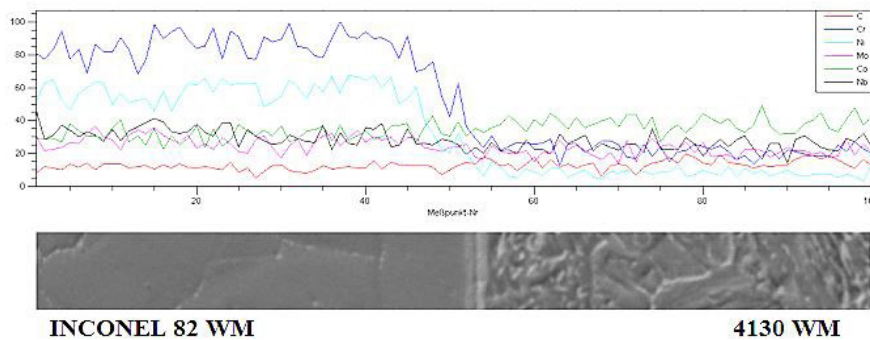
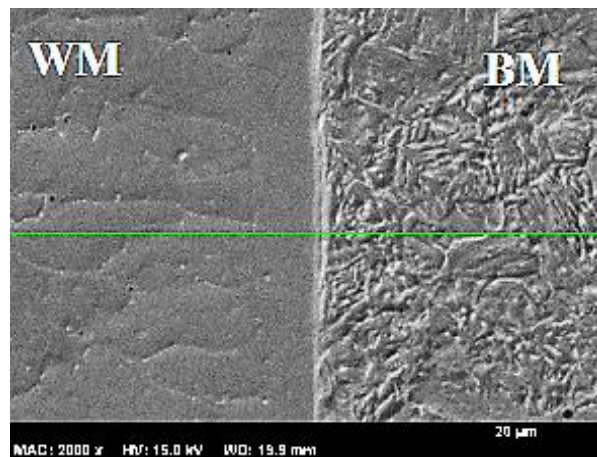


Fig. 10. EDS line analysis of the weld metal 4130 steel interface.

This drastic changes in alloying elements is indicative of unmixed zone in the interface.

The interface image between the weld metal and 316L base metal is shown in Figs. 11 and 12 The base metal consists of austenitic matrix and delta ferrite strings. twin boundaries in austenitic matrix are also seen. Also, the aggregation of lattice ferrite in HAZ and near the interface is observed. This can be caused by overheating in this area during welding. Aggregation of lattice ferrite leads to increase in the strength and hardness (Fig. 12), and decrease in flexibility in this area. The increase in

grain size of austenite is clear in HAZ. In the weld metal, cellular growth and also planar growth are observed in the neighbouring of the interface. This phenomenon is due to the high rate of heat transfer. Epitaxial growth is also partly visible in Fig. 11 (B).

In Fig. 12 epitaxial growth, SGB (Sub-grain boundaries) and GB (grain boundaries) are clearly seen due to the A type solidification mechanism. It should be noted that in this area carbide particles have been formed and cellular structure of the weld metal is the main characteristic of microstructure.

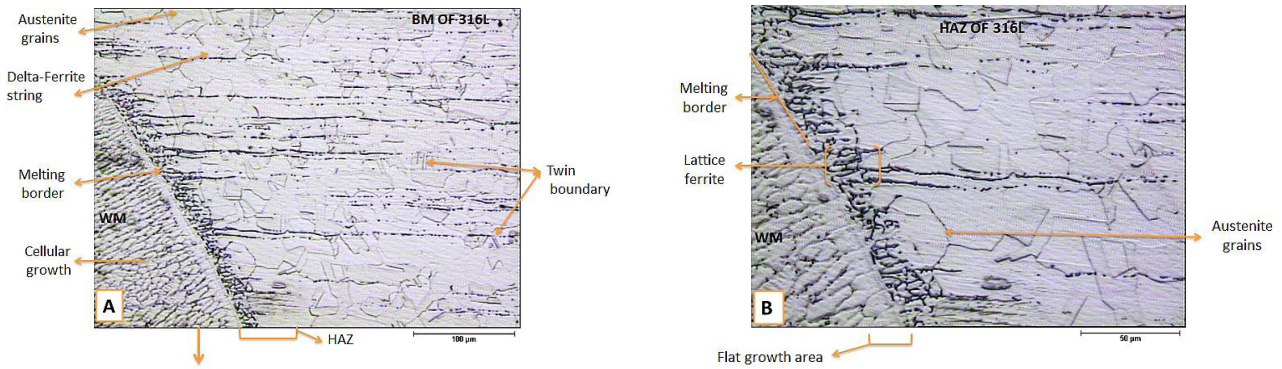


Fig. 11. The microstructure of 316L steel-weld metal interface at different magnifications.

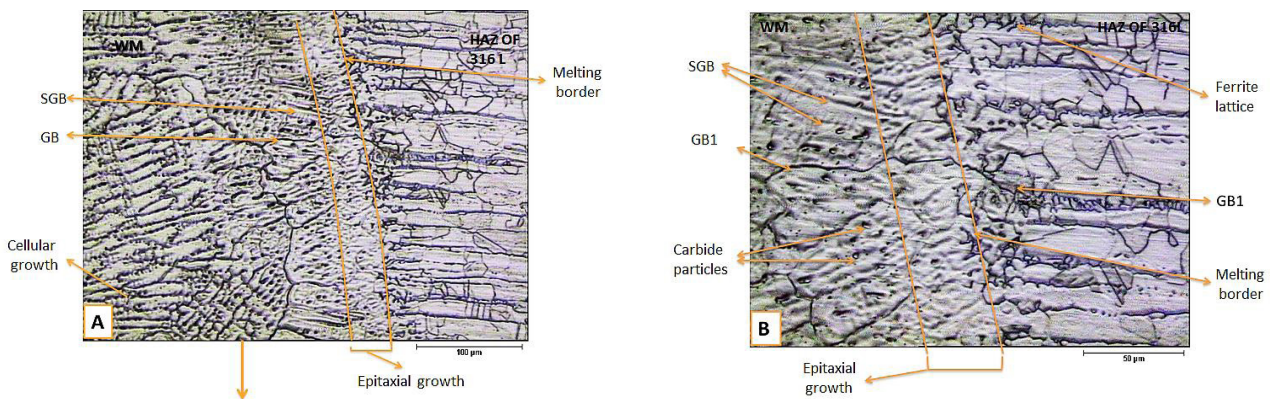


Fig. 12. The microstructure of 316L-weld metal interface at different magnifications.

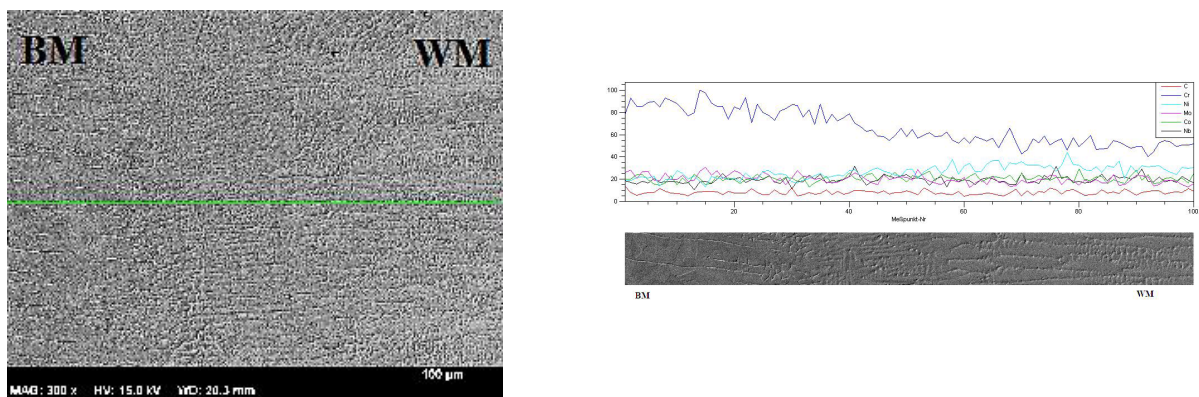


Fig. 13 EDS line analysis of the the weld metal-316L steel interface.

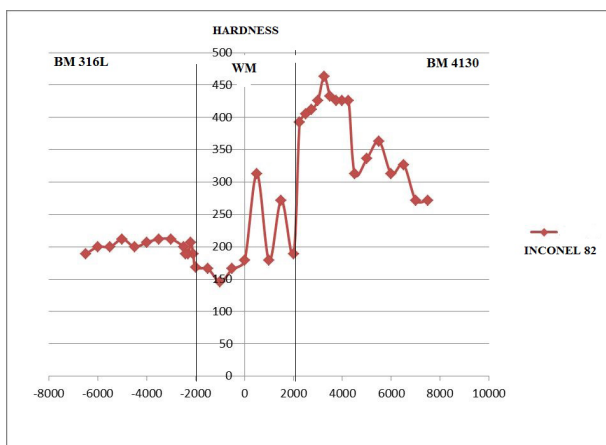


Fig.14. The microhardness diagram of the welded sample from different areas.

Aggregation of lattice ferrite in HAZ and in the vicinity of interface is also clearly seen.

To study the changes of alloying elements in the interface, the line scan was performed and the results are presented in Fig. 13. Small changes in alloying elements with gentle slope at diagram, especially in the chromium and nickel in the interface, is visible. This gentle slope changes in alloying elements is indicative of mixed zone in the interface.

Fig. 14 shows the microhardness profile of the welded sample. As shown, in the HAZ of 4130 steel, the microhardness increased compared to the base metal. According to Figs. 5, 6 and 7, it is due to the formation of martensite phase and also an increase in the amount of bainite structure in the HAZ area. In the weld zone a decrease in hardness value from AISI 4130 steel to AISI 316L can be seen. This reduction in microhardness can be due to the less amount of carbon in the weld area in the vicinity of the AISI 316L base metal<sup>17, 18, 19</sup>.

#### 4. Conclusions

The obtained results from this research work are summarized as follows:

- The weld metal had entirely austenitic microstructure with relatively equiaxed grains and dendritic morphology. Also the carbide particles were seen in the microstructure.
- Aggregation of the ferrite in HAZ of 316L base metal in the vicinity of the fusion boundary was seen due to the thermal conditions in this area.
- The grain growth in 316L steel-weld metal interface

was epitaxial due to the relatively similar chemical composition of the base and weld metals.

- The grain growth in 4130 steel-weld metal interface was unepitaxial due to the severe difference in the chemical composition of the base and weld metals.
- The welded sample indicated the highest microhardness in HAZ of 4130 steel because of the presence of tempered martensite and bainite in this area.

#### References

- [1] H. Ghazanfari, M. Naderi: *Acta Metall. Sin.*, 26(2013), 635.
- [2] N. Kumar, P. Bhaskar, Y. Mastanaiah, P. Murthy: *Procedia Mater. Sci.*, 5(2014), 2382.
- [3] S. Kou: *Welding Metallurgy*, 2nd ed., Wiley-interscience, Ney Jersey, USA, (2003)
- [4] L. Ying Li, Y. Wang, T. Han, L. Chao: *Inte. J. Mineral. Metall. Mater.*, 18(2011), 419.
- [5] J. Lippold, C. Kotecki, D. J.: *Welding Metallurgy and Weldability of Stanlees*, John Wiley & Sons Jercey Inc., New Jersey, USA, (2005).
- [6] E. Bain, C. Paxton, W. H.: *Alloyig Elements in Steel*, Second Edition, Third Revised Printing, American Society for Metal, USA, (1966).
- [7] N. Arivazhagan, S. Singh, S. Prakash, G. M. Reddy: *Mater. Design.*, 32(2011), 3036.
- [8] M. P. Reddy, A. A. S. William, M. M. Prashanth, S. N. S. Kumar, K. D. Ramkumar, N. Arivazhagan, S. Narayanan: *Procedia Eng.*, 75(2014), 29.
- [9] C. Jang, J. Lee, J. S. Kim, T. E. Jin: *Int. J. Pres. Ves. Pip.*, 85(2008), 635.
- [10] J. W. Kim, K. Lee, J. S. Kim, T. S. Byun: *J. Nucl. Mater.*, 384(2009), 212.
- [11] E. Ahmadi, A. R. Ebrahimi: *Adv. Mater. Proc.*, 1(2013), 55.
- [12] H. Mostaan, M. Shamanian, M. P. Monirvaghefi, S. Behjati, J. A. Szpunar, J. Sherafati: *Vacuum*, 109(2014), 148.
- [13] G. S. Chander, G. M. Reddy, G. R. N. Tagore: *Int. J. Adv. Manuf. Techn.*, 64(2013), 1445.
- [14] N. Özdemir, F. Sarsilmaz, A. Hasçalık: *Mater. Design.*, 28(2007), 301.
- [15] W. E. White, W. E. May: *Metallography*, 3(1970), 35.
- [16] A. V. Kington, F. W. Noble: *Mater. Sci. Eng.*, 138(1991), 259.
- [17] M. Poorkabirian, H. Mostaan, M. Rafiei: *J. Adv. Mater. Eng. (Esteghlal)*, 36(2017), 33.
- [18] S. Wang, Q. Ma, Y. Li: *Mater. Design.*, 32(2011), 831.
- [19] P. Bala Srinivasan, V. Muthupandi, W. Dietzel, V. Sivan: *Mater. Design.*, 27(2006), 182.